PRZEGLĄD ELEKTROTECHNICZNY

Ukazuje się od 1919 roku 6'14

Organ Stowarzyszenia Elektryków Polskich • Wydawnictwo SIGMA-NOT Sp. z o.o.

Piotr SOBAŃSKI, Teresa ORŁOWSKA-KOWALSKA

Wroclaw University of Technology, Institute of Electrical Machines Drives and Measurements

Voltage inverter IGBT fault diagnosis in the sensorless induction motor drive with MRAS^{CC} speed estimator

Abstract. *This article discusses the issue of a single IGBTs open-circuit fault diagnosis problem in voltage source inverters feeding modern electric motor drives. In the first stage of simulation tests the analysis of selected state variable transients relating to the field oriented controlled induction motor drive operation under inverter fault was presented, and then some simulation results of the modeled diagnostic system were introduced.*

Streszczenie. *W artykule omówiono problem diagnostyki uszkodzeń polegających na braku przewodzenia prądu jednego z tranzystorów falownika napięcia we współczesnych napędach elektrycznych. W pierwszej części badań symulacyjnych przeprowadzono analizę wybranych zmiennych stanu w bezczujnikowym napędzie indukcyjnym z bezpośrednim sterowaniem polowo zorientowanym, w którym przekształtnik uległ uszkodzeniu, a następnie przedstawiono wyniki testów zamodelowanego układu diagnostyki awarii. (**Diagnostyka awarii tranzystorów IGBT falownika napięcia w bezczujnikowym napędzie indukcyjnym z estymatorem prędkości typu MRAS^{CC}**)*

Keywords: sensorless drive, voltage inverter, IGBT faults diagnosis, speed estimator, MRAS
Słowa kluczowe: napęd bezczujnikowy, falownik napięcia, diagnostyka uszkodzeń łączników IGBT, estymator prędkości, MRAS.

doi:10.12915/pe.2014.06.01

Introduction

Nowadays induction motor (IM) drives are most frequently used in industry, mainly due to an intensive development of power electronics devices and vector control methods. These methods require state variable estimators, to perform very good dynamical performances of the drive systems. Moreover, extended requirements for cost and space minimization caused the development of different speed estimation methods, which have enabled the elimination of expensive encoders or resolvers in the AC drive systems [1-9]. The developed different speed estimation methods for AC motor drives, presented in the literature, can be divided into three groups:

– methods based on a signal injection (usually a high frequency signal); this additional signal modulated by a natural anisotropy of a machine is contained in a measured stator current signal, and after suitable analysis can be used for the rotor speed determination [3, 4];
– algorithms based on an analytical model of a controlled machine, like: state observers [1-3, 5] Kalman filters [2, 6], or model-based adaptive algorithms of MRAS-type [2, 7]. These last are very popular and are based on a minimization of an error between the output signals of different state estimators (flux, current, reactive power etc.);
– artificial intelligence techniques, which use neural networks of different structures [2, 8, 9], and do not need the mathematical model or parameters knowledge of AC motors.

A simple construction and low costs of an IM as well as a possibility of a speed sensor elimination caused, that IM drives are the most reliable drives applied in industry. However, different faults can sometimes occur in a drive, among them static converter faults. More than half of these faults are connected with the static switches short-circuits or open-switch faults [10]. In case of drive systems with speed sensor, a suitable fault localization procedure enables an action which limits or minimizes fault effects and preserves relatively high functionality of the drive system [11]. On the other hand, in case of sensorless drives, an influence of the voltage inverter faults on a drive system operation and its functionality is not often investigated [12] and should be widely analyzed.

Open-switch faults diagnosis techniques can be based on the analysis of easily accessible signals, namely current or voltage. In the most effective methods additional inverter voltage sensors are used. Some interesting results have been presented in [13]-[16], where open-switch fault localization algorithms, based on a comparison between different measured and calculated voltages of an inverter have been verified experimentally. Due to the requirement of additional voltage sensors, these methods generate additional implementation costs and are not popular in industrial applications. Thus, in the last years, new diagnostic algorithms, that are based on normally used in a control structure state variables, have been developed. For example, in the paper [17], localization of the faulted transistor switch is realized using comparison of average values of estimated phase voltages of a motor with average voltage reference signals.

The second group of the open-switch diagnostic methods is based on stator phase currents measurements. The most frequently proposed algorithms rely on an analysis of the stator current vector hodograph in the α–β complex plane [18]. The detailed overview of these techniques is presented in [19]. Opposite to the voltage-based diagnostic methods, a fault localization time of the algorithms based on the stator phase current measurements is longer than one current period. It causes that motor can be stalled before a suitable fault remedial action will be taken on. This problem occurs especially in the low speed range of a nominally loaded motor [20].

However, all mentioned methods have been tested in AC motor drives with speed sensor only. In this paper a simple and fast voltage-based fault detection method has been applied to the sensorless direct field-oriented control method (DFOC) of an induction motor drive. The effectiveness of this method was tested in simulation for different operation conditions of the drive system. Some modification of the fault detection method suitable for the sensorless control structure has been proposed. Simulation tests were realized in MATLAB/Simulink, using PL-Grid infrastructure.

Fault diagnosis of voltage inverter in the sensorless drive

Based on the short overview of the most popular diagnosis methods of voltage inverter faults given in the Introduction, the method presented in [17] has been chosen for the application in the sensorless IM drive. This method is very fast and does not require additional implementation costs. The method described in [17] has been originally tested in the PMSM drive. It is based on the calculation of the difference between estimated values of stator phase voltages $u_{sf\,est}$ and their reference values $u_{sf\,ref}$. This error is next normalized with the DC bus voltage U_{DC} according to:

$$d_f = \left\langle \frac{u_{sf\,ref} - u_{sf\,est}}{U_{DC}} \right\rangle, \tag{1}$$

where: $f=A,B,C$.

Stator phase voltages of an IM can be estimated using the mathematical model of the stator winding [2], recalculated to the following form [p.u.]:

$$\mathbf{u}_s^{\alpha-\beta} = \frac{x_m T_N}{x_r}\frac{d}{dt}\boldsymbol{\psi}_r^{\alpha-\beta} + r_s \mathbf{i}_s^{\alpha-\beta} + \sigma x_s T_N \frac{d}{dt}\mathbf{i}_s^{\alpha-\beta}, \tag{2}$$

after Clark – Park transform:

$$\begin{aligned} u_{sA} &= u_{s\alpha} \\ u_{sB} &= -\frac{1}{2}u_{s\alpha} + \frac{\sqrt{3}}{2}u_{s\beta} \\ u_{sC} &= -\frac{1}{2}u_{s\alpha} - \frac{\sqrt{3}}{2}u_{s\beta} \end{aligned} \tag{3}$$

The following notation was used above: $\mathbf{u_s}$, $\mathbf{i_s}$, $\boldsymbol{\psi}_\mathbf{r}$ – stator voltage, current and rotor flux vectors in the $\alpha-\beta$ stationary reference frames, r_s, x_s, r_r, x_r – stator and rotor winding resistances and reactances, x_m – main reactance, $\sigma=1-x_m^2/(x_s x_r)$, f_{sN} – nominal stator frequency, $T_N=1/(2\pi f_{sN})$.

The rules of fault localization algorithm for the two-level voltage inverter (Fig. 1), proposed in [17], are given in the Table 1. These rules have been extended here with additional conditions which enable proper operation of the IM speed-sensorless drive. The threshold value k_d has been determined experimentally as k_d=0.28 p.u., to avoid false alarms.

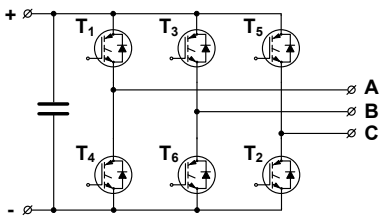

Fig. 1. Scheme of the power circuit of two-level voltage inverter

Table 1. Rules of the fault localization algorithm

Faulted transistor	d_A	d_B	d_C
T_1	$>k_d$	$<-k_d$	$<-k_d$
T_2	$>k_d$	$>k_d$	$<-k_d$
T_3	$<-k_d$	$>k_d$	$<-k_d$
T_4	$<-k_d$	$>k_d$	$>k_d$
T_5	$<-k_d$	$<-k_d$	$>k_d$
T_6	$>k_d$	$<-k_d$	$>k_d$

Mathematical model of the stator current-based MRAS^{CC} estimator

The stator-current based speed estimator MRAS^{CC} has been described and widely tested in [7]. This estimator contains two mathematical models: a rotor-flux-model based on measured stator currents, and a stator-current-model based on measured stator currents and voltages. Both models are adjusted by an estimated rotor speed value, as it is shown in Fig. 2.

The stator-current model and respectively the rotor-flux-model are described by the following equations in p.u. system [2, 7]:

$$\begin{aligned} \frac{d}{dt}\mathbf{i_{s\,est}} = &-\frac{r_r x_m^2 + x_r^2 r_s}{\sigma T_N x_s x_r^2}\mathbf{i_{s\,est}} + \frac{1}{\sigma T_N x_s}\mathbf{u_s} + \\ &+ \frac{x_m r_r}{\sigma T_N x_s x_r^2}\boldsymbol{\psi}_{\mathbf{r\,est}} - j\omega_{m\,est}\frac{x_m}{\sigma T_N x_s x_r}\boldsymbol{\psi}_{\mathbf{r\,est}} \end{aligned} \tag{4}$$

$$\frac{d}{dt}\boldsymbol{\psi}_{\mathbf{r\,est}} = \left[\frac{r_r}{x_r}\left(x_m \mathbf{i_s} - \boldsymbol{\psi}_{\mathbf{r\,est}}\right) + j\omega_{m\,est}\boldsymbol{\psi}_{\mathbf{r\,est}}\right]\frac{1}{T_N} \tag{5}$$

where: $\mathbf{i_{s\,est}}$, $\boldsymbol{\psi}_{\mathbf{r\,est}}$ – estimated stator current and rotor flux vectors, $\omega_{m\,est}$ – estimated rotor speed.

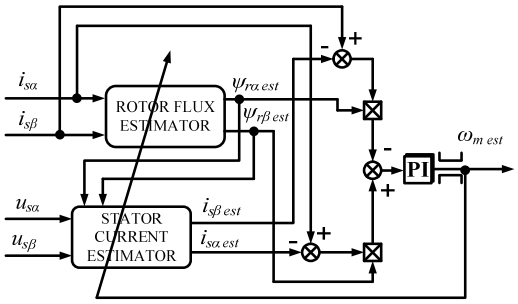

Fig.2. Block scheme of the MRAS^{CC} speed estimator [7]

Based on a stator current estimation error $e_{is\alpha,\beta}$, defined as follows:

$$e_{is\alpha,\beta} = i_{s\alpha,\beta} - i_{s\alpha,\beta\,est}, \tag{6}$$

a rotor speed is calculated using the adaptive algorithm [7]:

$$\begin{aligned} \omega_{m\,est} = &K_P\left(e_{is\alpha}\psi_{r\beta\,est} - e_{is\beta}\psi_{r\alpha\,est}\right) + \\ &+ K_I\int\left(e_{is\alpha}\psi_{r\beta\,est} - e_{is\beta}\psi_{r\alpha\,est}\right)dt. \end{aligned} \tag{7}$$

Stator current estimation requires knowledge of the voltage components $u_{s\alpha,\beta}$ (Fig.2), which are usually estimated basing on the switching signals for inverter's IGBTs [7]. However, under IGBT switches faults, such solution gives incorrect information on $u_{s\alpha,\beta}$ and can not be longer applied,

because an output voltage of the inverter commanded by the control system can not be obtained due to the fault. In such situation the speed estimation process is not properly realized. Thus under faulty condition of inverter's switches in a speed-sensorless IM drive, a stator voltage can not be estimated but has to be measured. In the next part of the paper such two cases have been investigated.

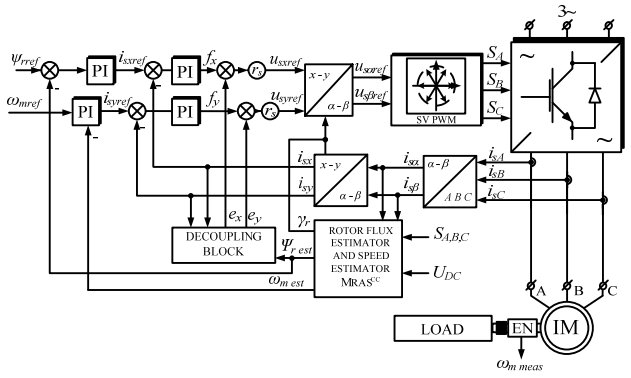

Fig.3. Block scheme of the DFOC structure for the IM sensorless drive with MARS^{CC} estimator of the rotor flux and speed

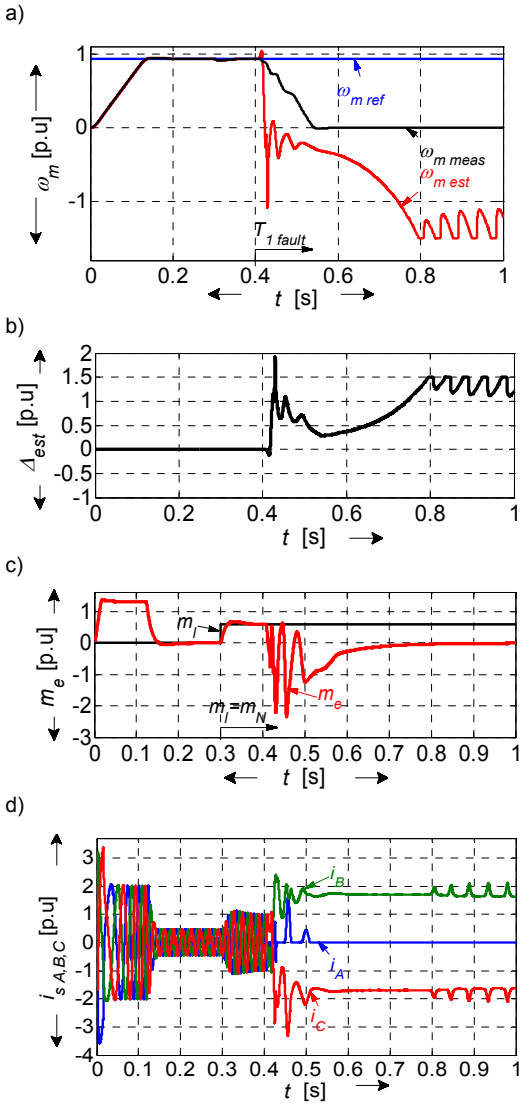

Fig.4. Transients of the motor speeds ω_m (a), speed estimation error Δ_{est} (b), electromagnetic torque m_e (c) and stator phase currents $i_{sA,B,C}$ (d) under transistor T1 fault and stator voltage calculated using logic control signals of IGBTs; $\omega_m = \omega_N$, $m_l = m_N$

Simulation results

The block scheme of tested DFOC induction motor drive, presented in Fig. 3, has been modeled using MATLAB/Simulink. The simulation model of the voltage inverter with suitable stabilization of the DC bus voltage (a vector control structure for an active rectifier) was developed using elements of the SimPower System library [19, 20]. The IGBT open-switch faults were realized by applying 0 signal to the suitable transistor gate [20]. The basic parameters of the drive are shown in Table 2 (Appendix).

In the following figures all main state variables of the drive system are presented, like: the reference $\omega_{m\,ref}$, measured $\omega_{m\,meas}$ and estimated rotor speeds (Fig. 4a, 5a), the speed estimation error (Fig. 4b, 5b) given by the expression:

$$\Delta_{est} = \omega_{m\,meas} - \omega_{m\,est} \,. \tag{8}$$

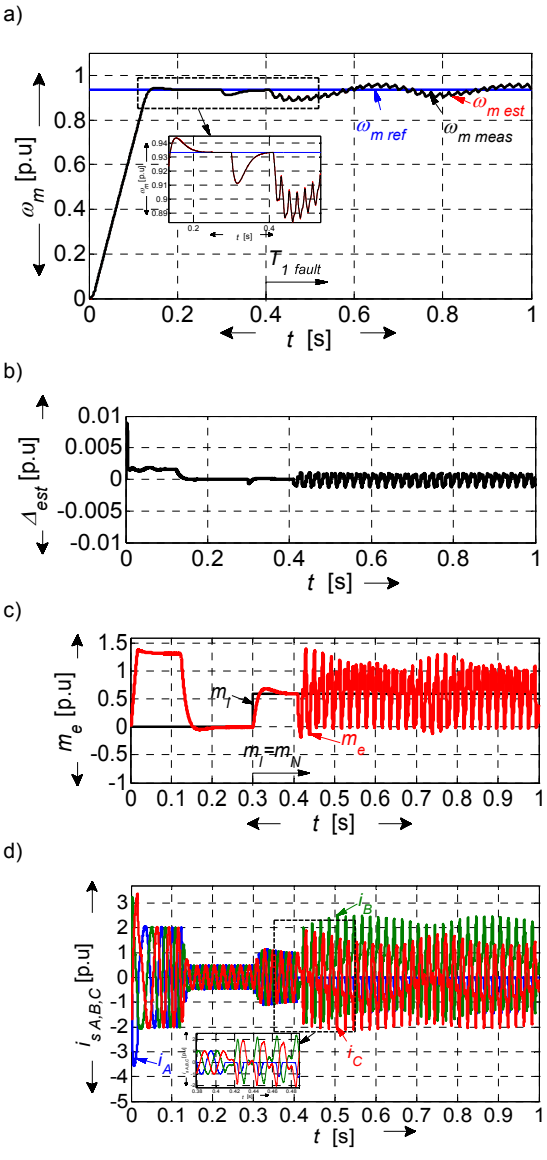

Fig.5. Transients of the motor speeds ω_m (a), speed estimation error Δ_{est} (b), electromagnetic torque m_e (c) and stator phase currents $i_{sA,B,C}$ (d) under transistor T1 fault and measured stator voltage $u_{sA,B,C}$; $\omega_m = \omega_N$, $m_l = m_N$

Next the electromagnetic torque m_e and load torque m_l (Fig. 4c, 5c) and stator phase currents $i_{sA,B,C}$ (Fig. 4d, 5d) are presented. It should be mentioned, that the measured speed was only used for a comparison with the estimated one and

the error (8) calculation (see Fig. 3). In the time t=0.4s the transistor T1 fault was simulated, which is marked in Fig. 4 and Fig. 5 as $T_{1\,fault}$. Additionally a time when the nominal load torque m_l=m_N was applied to the motor are marked there.

The chosen simulation results of the sensorless drive operation under open-switch fault of the voltage inverter are demonstrated in the Fig. 4. In these tests the stator voltage, required for the MRAS^{CC} speed estimator has been calculated based on the logic control signals of the transistor gates, given by the SVM modulator, like in [7].

The tests of the sensorless IM drive with MRAS^{CC} estimator, based on the stator voltage calculated using logic control signals of the inverter switches, accessible in the FOC structure, show that under IGBT open-switch fault a stable operation of the drive system is not possible (Fig. 4a). In a short time after fault occurrence the real IM speed reaches zero value, the speed estimation error takes maximal value (Fig. 4b), which is limited by the saturation of PI controller in the speed adaptation algorithm (7) of this estimator.

Thus, in the next test, the stator phase voltage $u_{sA,B,C}$. measurements were assumed and taken to the speed estimation algorithm. The drive system behavior with these measurement applied in the MRAS^{CC} estimator is shown in Fig. 5. In this figure, the drive transients under T1 transistor fault has been demonstrated, but the drive performance are the same under other cases of the single open-switch faults. Similarly to the test results presented in the earlier work of the authors [20], in the low speed range ω_m <0,25ω_N, the drive will stop under any transistor switch failure. However, the application of the phase voltage measurement sensors provides the stability of the speed estimation algorithm based on the stator voltage information. It is visible, that for such solution, the speed estimation algorithm enables the operation of the drive system under the open-switch fault of the inverter, similarly as for a IM drive with speed sensor (this case has been tested in [20]). However, relatively the large torque oscillations occur (Fig. 5c) and they could be dangerous for a mechanical coupling, so the drive operation should not be continued too long. The functionality of the drive is lower, but it can operate as long as the safe switch-off will occur.

In both analyzed speed-sensorless solutions, with and without stator voltage measurements, the time requirements for the open-switch fault detection and localization are quite different. The information on real voltage $u_{sA,B,C}$ values enables the proper speed signal $\omega_{m\,est}$ estimation (Fig. 5a,b) and keeping the average value of the real motor speed on the reference level. Thus, the time required for the fault localization before the drive system stop, is much longer. However, such solution increases implementation costs of the control structure, which could limits its industrial applications. Thus it is reasonable to apply fast fault diagnostic algorithms, which enable the localization of the fault before an uncontrolled drive stall.

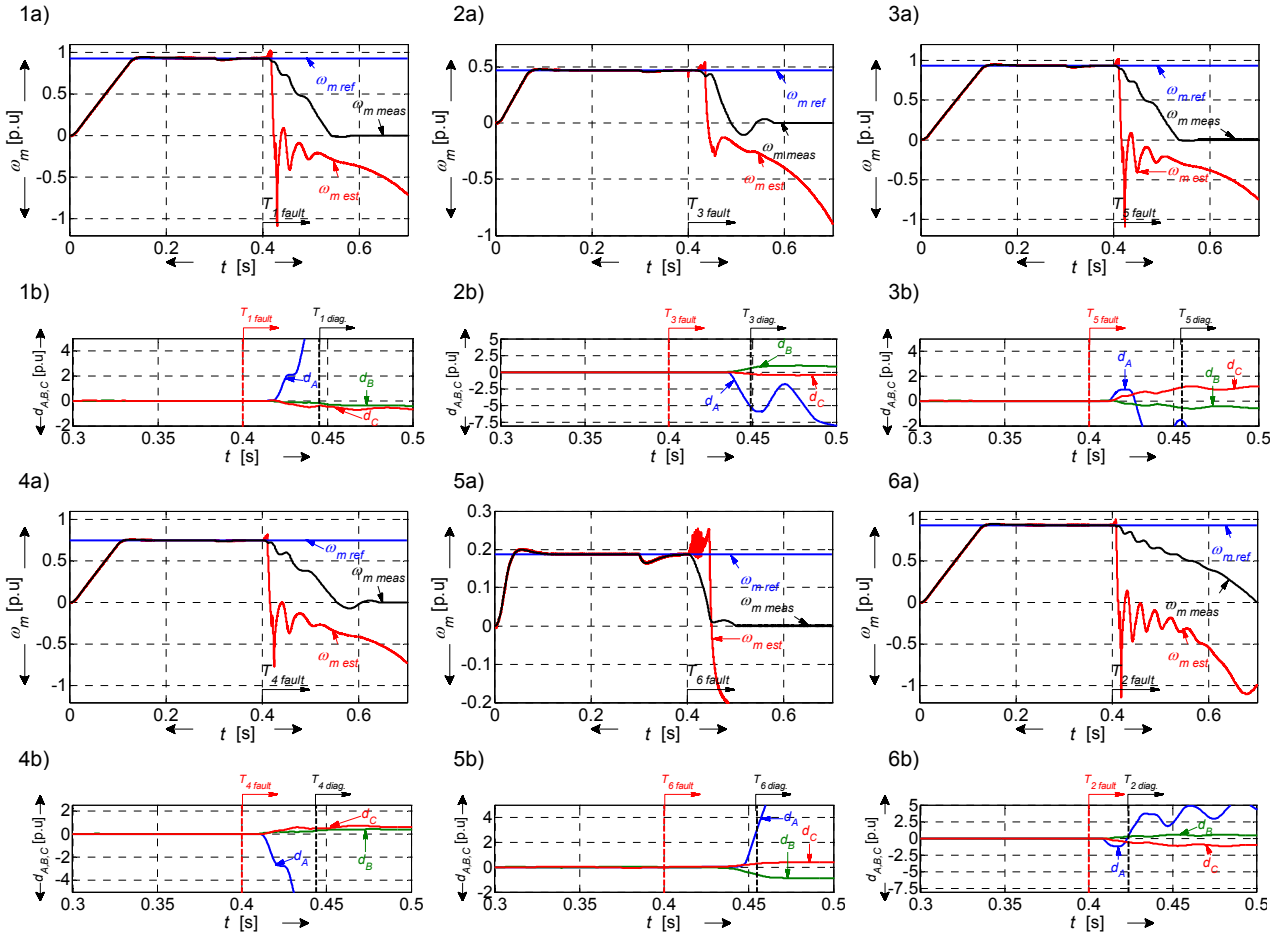

Fig. 6. Transients of the rotor speed ω_m and diagnostic signals $d_{A,B,C}$ under: T1 transistor fault for ω_m=ω_N and m_l=m_N (1a, b), T3 transistor fault for ω_m=0,5ω_N and m_l=0,5m_N (2a, b), T5 transistor fault for ω_m=ω_N and m_l=m_N (3a, b), T4 transistor fault for ω_m=0,8ω_N and m_l=0,3m_N (4a, b), T6 transistor fault for ω_m=ω_N and m_l=m_N (5a, b), T2 transistor fault for ω_m=ω_N and m_l=m_N (6a, b)

In the last part of research, the open-switch fault diagnostic method described in this paper has been tested under wide range of the motor speed and load torque. In Fig. 6 the actual and estimated motor speeds are presented in the same way as before. Moreover, the diagnostic signals $d_{A,B,C}$ (1) are presented, as well as times of: certain switch faults $T_{n\,fault}$ and faults identification $T_{n\,diag.}$, while n=1,...,6 refers to the transistor number according to Fig.1.

The examples of tests presented in Fig. 6 confirm the effectiveness of the tested diagnostic method with some additional rules given in the Table 1, in the wide range of the drive speed reference and load values. In each tested case, the fault localization has occurred before the motor stall. Comparing to the original diagnostic algorithm [17], which has been tested in the drive with speed measurement only, the faulted transistor localization procedure was based on independent monitoring of diagnostic signals d_f. This led to simple monitoring system and faster identification of the faulted transistor. However, as it can be seen in Fig. 6, when the transistors T5 or T2 are damaged, such solution cause the wrong diagnosis, because under simulated fault signal d_A has changed its sign twice. Moreover, in all presented situations the growth of d_A signal is the biggest, which also cause the diagnostic error in case of the simplified algorithm. Using the method propose in this paper, the wrong diagnoses (false alarms) are eliminated.

Conclusions

The analysis of sensorless DFOC induction motor drive with *MRAS*^{CC} speed estimator under voltage inverter faults was presented in this paper. It was shown that the proposed diagnostic methods of the open-switch faults, extended with the additional rules (comparing to [17]) is reliable and fast enough to detect the transistor fault occurrence and localization. It was proved that the speed estimator, that is based on the stator voltage measurement, is able to provide a safe operation of the sensorless drive system under speed reference value ω_m>0.25ω_N, similarly as in a case of a drive with speed sensor.

APPENDIX

Table 2. Nominal parameters of the tested IM drive

Power P_N [kW]	1.1
Stator voltage U_N [V]	220/380
Stator current I_N [A]	2.9/5
Rotor speed n_N [rev/min]	1400
Stator frequency f_N [Hz]	50
Poles pair number p_b [-]	2

This research work was supported by National Science Centre (Poland) under project DEC-2013/09/B/ST7/04199

REFERENCES

[1] Finch J.W., Giaouris D., Controlled AC Electrical Drives, *IEEE Trans. Industrial Electronics*, 55 (2008), n.2, 481-491

[2] Orlowska–Kowalska T., Sensorless Induction Motor Drives, *Wroclaw University of Technology Press*, Wroclaw, (2003)

[3] Holtz J., Sensorless Control of Induction Machine – With or Without Signal Injection?, *IEEE Trans. Industrial Electronics*, 53 (2006), n.1, 7-30

[4] Yoon Y., Sul S., Morimoto S., Ide K., High Bandwidth Sensorless Algorithm for AC Machines based on Square-wave Type Voltage Injection, *IEEE Energy Conversion Congress and Expo*, 47 (2011), n.3, 1361-1370

[5] Krzeminski Z., A new speed observer for control system of induction motor, *IEEE Int. Conf. on Power electronics and Drive Systems, PESC'99, Hong Kong, 1999*

[6] Auger F., Guerrero J., Hilairet M, Monmasson E., Orlowska-Kowalska T. and Katsura S., Industrial Applications of the Kalman Filter: A Review, *IEEE Trans. on Industrial Electronics*, 60 (2013), n.12, 5458-5471

[7] Orlowska-Kowalska T, Dybkowski M., Stator Current-based MRAS Estimator for Wide Range Speed-Sensorless Induction Motor Drive, *IEEE Trans. Industrial Electronics*, 57 (2010), n.4, 1296 – 1308

[8] Cirrincione M., Pucci M., Cirrincione G., Capolino G.A., Sensorless control of induction machines by a new neural algorithm: The TLS EXIN neuron, *IEEE Trans. on Industrial Electronics*, 54 (2007), n.1, 127-149.

[9] Grzesiak L., Ufnalski B., Projektowanie neuronowego estymatora prędkości kątowej silnika indukcyjnego przy zastosowaniu analizy składowych głównych, *Przegląd Elektrotech*., (2004), nr 5, 493-497

[10] Yang S., Xiang D., Bryant P., Ran L., Tavner P., Condition monitoring for device reliability in power electronic converters: a review, *IEEE Trans. on Power Electronics*, 25 (2010), 2734-2752

[11] Ribeiro R.L.A., Jacobina C.B., Lima A.M.N., DA Silva E.R.C., A Strategy for Improving Reliability of Motor Drive Systems Using a Four-Leg Three-Phase Converter, *Proc. 16th Ann. IEEE Applied Power Electronics Conf. and Expo*., Anaheim, 1 (2001), 385-391

[12] Trabelsi M., Jouili M., Boussak M. Koubaa Y., Gossa M., Robustness and limitations of sensorless technique based on Luenberger state-observer for induction motor drives under inverter faults, *IEEE Int. Symp. on Industrial Electronics ISIE'2011*, Gdansk, Polnad, (2011), 716-721

[13] Araujo Ribeiro R.L., Jacobina C.B., Cabral da Silva E.R., Lima A. M.N., Fault detection of open-switch damage in voltage-fed PWM motor drive systems, *IEEE Trans. Power Electronics*, 18 (2004), 439-446

[14] Trabelsi M., Boussak M., Mestre P., Gossa M., An improved diagnosis technique for IGBTs open-circuit fault in PWM-VSI-fed induction motor drive, *IEEE Int. Symp on Ind. Electronics ISIE'2011,* Gdansk, Poland, (2011), 2111-2117

[15] Lee Choi C,W., Design and evaluation of voltage measurement based sectoral diagnosis method for inverter open switch faults of permanent magnet synchronous motor drives, *IET–Electric Power Applications*, 6 (2012), 526-532

[16] Jung Shin-Myung, Park Jin-Sik, Kim Hyoung-Suk, Kim Hag-Wone, Youn Myung-Joong, Simple switch open fault detection method of voltage source inverter, *Energy Conversion Congress and Exposition IEEE*, (2009), 3175-3181

[17] Freire N.M.A., Estima J.O., Cardoso A.J.M., A voltage-based approach for open-circuit fault diagnosis in voltage-fed SVM motor drives without extra hardware, *XXth Int. Conf. on Electrical Machines*, (2012), 2378-2383

[18] A.M.S. Mendes, A.J. Marques Cardoso, Voltage source inverter fault diagnosis in variable speed AC drives, by the average current Park's vector approach, *Int. Conf. on Electr. Mach. and Drives*, (1999), 704-706

[19] Sobański P., Orłowska-Kowalska T., Metoda diagnostyki uszkodzenia typu przerwa łącznika IGBT falownika napięcia w układzie wektorowego sterowania silnikiem indukcyjnym, *Przegląd Elektrotechniczny,* 89 (2013),nr 6, 159-163

[20] Sobański P., Orłowska-Kowalska T., Wpływ uszkodzenia tranzystora IGBT falownika napięcia na przebiegi zmiennych stanu silnika indukcyjnego ze sterowaniem wektorowym, *Przegląd Elektrotechniczny,* 89 (2013),nr 2b, 162-165

Authors:
Piotr Sobański, M.Sc., Teresa Orłowska-Kowalska, D.Sc., Ph.D., Prof., Wrocław University of Technology, Institute of Electrical Machines, Drives and Measurements, ul. Wybrzeże Wyspiańskiego 27, 57-370 Wrocław, piotr.sobanski@pwr.wroc.pl, teresa.orlowska-kowalska@pwr.wroc.pl